

Magneto-optical Kerr rotation enhancement in Co-ZnO inhomogeneous magnetic semiconductor

Y. P. Zhang, Shi-Shen Yan,^{a)} Yi-Hua Liu, Miao-Juan Ren, Y. Fang, Y. X. Chen, G. L. Liu, and L. M. Mei
School of Physics and Microelectronics, Shandong University, Jinan, Shandong 250100, People's Republic of China

J. P. Liu
Department of Physics, The University of Texas at Arlington, P.O. Box 19059, Arlington, Texas 76019

J. H. Qiu, S. Y. Wang, and L. Y. Chen
Department of Optical Science and Engineering, Fudan University, Shanghai 200433, People's Republic of China

(Received 27 October 2005; accepted 19 June 2006; published online 24 July 2006)

The polar Kerr rotation and ellipticity spectra of the as-deposited and annealed $\text{Zn}_{1-x}\text{Co}_x\text{O}$ inhomogeneous magnetic semiconductors were measured. The Kerr rotation spectra versus the photon energy can be greatly modulated by adjusting the Co concentration or annealing the samples. Moreover, the observed maximal Kerr rotation, 0.72° , in an annealed sample is higher than that of pure Co films, Pt/Co multilayers, and $\text{Pt}_x\text{Co}_{1-x}$ alloys. The enhanced Kerr rotation in the annealed samples can be explained by the fact that the annealed samples became a nanocomposite system consisting of Co clusters and $\text{Zn}_{1-x}\text{Co}_x\text{O}$ magnetic semiconductor. © 2006 American Institute of Physics. [DOI: 10.1063/1.2234280]

Recently magnetic semiconductors (MSs) have attracted considerable attention because of their potential applications in photoelectronics, magnetoelectronics, and microwave devices.^{1,2} Since high optical transparency of ZnO in the visible light range along with good electrical conductivity can be achieved by appropriate impurity doping, the doped ZnO can be used as transparent electrodes in solar cells and flat panel display. The doped ZnO and ZnO-based heterostructures can also be used in the photoelectronic devices such as light-emitting and laser diodes. To date, many studies have been done on the ZnO-based MSs, and room temperature ferromagnetism has been found by some groups.³⁻⁵ Since ZnO is a semiconductor with a wide band gap, ZnO-based MSs with room temperature ferromagnetism would be very useful for the short wavelength magneto-optical applications. Ando *et al.*^{6,7} and Jin *et al.*⁸ have reported a large magneto-optical effect [magnetic circular dichroism (MCD)] in the $\text{Zn}_{1-x}\text{Co}_x\text{O}$ magnetic semiconductor with a low doping level of Co, but no ferromagnetism was found in their samples.

However, the magneto-optical effects in the ferromagnetic semiconductor are still less known to date. In this letter, we report the magneto-optical Kerr effect in the as-deposited and annealed $\text{Zn}_{1-x}\text{Co}_x\text{O}$ inhomogeneous magnetic semiconductors with room temperature ferromagnetism. Moreover, the Kerr rotation spectra versus the photon energy can be greatly modulated by adjusting the Co concentration or by annealing samples.

The $\text{Zn}_{1-x}\text{Co}_x\text{O}$ MS films were prepared on glass substrates by alternately sputtering very thin Co layers and ZnO layers for 60 periods (the nominal structure is $[\text{Co } 0.6 \text{ nm}/\text{ZnO } y \text{ nm}]_{60}$) in Ar and background O_2 gas at room temperature. Changing the nominal thickness y in the

$[\text{Co } 0.6 \text{ nm}/\text{ZnO } y \text{ nm}]_{60}$ structure, $\text{Zn}_{1-x}\text{Co}_x\text{O}$ MSs with different compositions were obtained due to the interdiffusion during the growth ($y=0.3, 0.5, \text{ and } 1 \text{ nm}$ corresponding to $x=0.81, 0.72, \text{ and } 0.56$ in the $\text{Zn}_{1-x}\text{Co}_x\text{O}$, respectively). Detailed growth procedure, microstructures and magnetic properties of $\text{Zn}_{1-x}\text{Co}_x\text{O}$ inhomogeneous MSs were reported previously.³

The as-deposited samples were then annealed in a vacuum at 400°C for 2 h. Due to much higher Co concentration in the as-deposited samples than the solubility limit of Co in ZnO in the thermal equilibrium state, partial Co atoms could separate out from the $\text{Zn}_{1-x}\text{Co}_x\text{O}$ MSs to form Co clusters after annealing, and the samples developed into an inhomogeneous system consisting of ferromagnetic Co clusters of high magnetization and ferromagnetic $\text{Zn}_{1-x}\text{Co}_x\text{O}$ MS matrix of low magnetization. This was confirmed by x-ray diffraction and transmission electron microscope. The results of x-ray diffraction on as-deposited and annealed samples are shown in Fig. 1(a). For the as-deposited samples, no peaks are found since x-ray diffraction is not sensitive to the nanocrystal grains of 4–5 nm in diameter. After annealing, obvious peaks of hcp Co (0002) occurred. Other peaks marked as

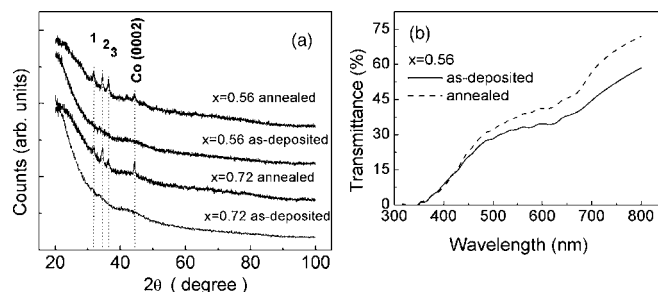


FIG. 1. (a) X-ray diffraction spectra of the as-deposited and annealed $\text{Zn}_{1-x}\text{Co}_x\text{O}$ films for $x=0.56$ and 0.72 , respectively. (b) Transmittance of the $\text{Zn}_{0.44}\text{Co}_{0.56}\text{O}$ films vs wavelength in the visible light region.

^{a)} Author to whom correspondence should be addressed; FAX: +86-531-88377031; electronic mail: shishenyan@yahoo.com

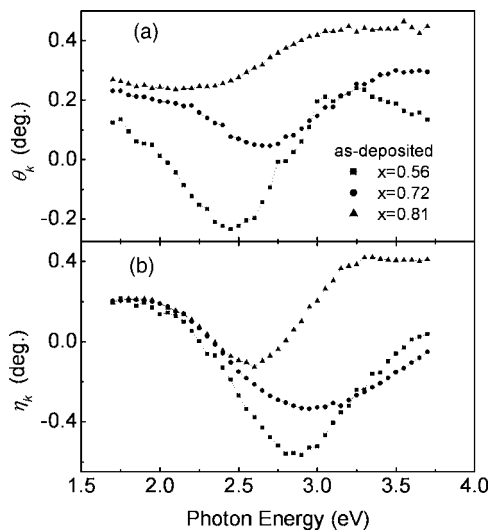


FIG. 2. The polar Kerr rotation θ_k (a) and the Kerr ellipticity η_k (b) of the as-deposited $\text{Zn}_{1-x}\text{Co}_x\text{O}$ MS samples measured in an external field of 1.1 T.

1, 2, and 3 in Fig. 1(a) come from the remanent $\text{Zn}_{1-x}\text{Co}_x\text{O}$ matrix, which are close to hcp ZnO ($10\bar{1}0$), (0002), and ($10\bar{1}1$), respectively.

The photon transmission spectrum of the as-deposited and annealed $\text{Zn}_{0.44}\text{Co}_{0.56}\text{O}$ samples is shown in Fig. 1(b). The films are half transparent in the visible light region and the transmittance decreases with decreasing light wavelength and falls to zero at 347 nm. The energy band gap of the as-deposited $\text{Zn}_{0.44}\text{Co}_{0.56}\text{O}$ is calculated to be 3.44 eV, which is close to that of pure ZnO films. The photon transmission spectra only show a slight enhancement after annealing.

Ando *et al.* and Jin *et al.* have reported $\text{Co}^{2+} d-d^*$ transitions near 2.0 eV in the $\text{Zn}_{1-x}\text{Co}_x\text{O}$ magnetic semiconductor.^{6,8} In our samples, a shoulder in the range of 500–600 nm (2.0–2.4 eV) is observed on the transmittance curve in Fig. 1(b), which is similar to that obtained in the $\text{Zn}_{1-x}\text{Co}_x\text{O}$.^{6,8} On the other hand, though pure Co clusters were not observed in the as-deposited samples, there may be Co-rich $\text{Zn}_{1-x}\text{Co}_x\text{O}$ and ZnO-rich $\text{Zn}_{1-x}\text{Co}_x\text{O}$ areas on the subnanometer scale, which was introduced by the alternate deposition and thermal nonequilibrium growth process. The inhomogeneity on the subnanometer scale may introduce many defect energy levels in the band gap and change the ZnO energy band structures. Therefore optical absorption due to the interband transitions from defect energy levels can be seen in a wide photon energy range.

The polar Kerr rotation θ_k and Kerr ellipticity η_k were recorded at room temperature on a magneto-optical Kerr spectrometer under an applied field of 11 kOe perpendicular to the film plane. A 150 W Xe short-arc lamp was used as a continuous light source covering a 1.7–3.7 eV spectral range. The measured polar Kerr rotation and Kerr ellipticity spectra were plotted in Figs. 2(a) and 2(b) for as-deposited $\text{Zn}_{1-x}\text{Co}_x\text{O}$ MS films with different Co concentrations. Figures 2(a) and 2(b) indicate that the Kerr spectra can be strongly modulated by adjusting the Co concentration. In Fig. 2(a), as the photon energy increases, θ_k of $\text{Zn}_{0.19}\text{Co}_{0.81}\text{O}$ increases after a small decrease in the low energy region, and θ_k of $\text{Zn}_{0.28}\text{Co}_{0.72}\text{O}$ decreases in the lower energy region from 1.7 to 2.7 eV and increases beyond 2.7 eV. However, θ_k of $\text{Zn}_{0.44}\text{Co}_{0.56}\text{O}$ is negative from 2.0 to 2.8 eV. The

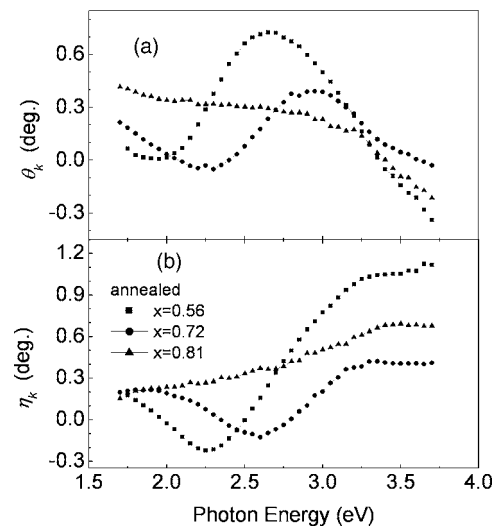


FIG. 3. The polar Kerr rotation θ_k (a) and the Kerr ellipticity η_k (b) of the annealed $\text{Zn}_{1-x}\text{Co}_x\text{O}$ MS samples measured in an external field of 1.1 T.

maxima of θ_k are 0.45° , 0.3° , and 0.24° for $x=0.81$, 0.72, and 0.56, respectively, and they all appear in the high photon energy region. In Fig. 2(b), η_k of the samples shows negative peaks at 2.6, 2.95, and 2.85 eV for $x=0.81$, 0.72, and 0.56, respectively. It is found that the photon energy dependences of the Kerr effect spectra for various Co concentrations are different from those of pure Co,^{9–11} which implies that the magneto-optical Kerr effect of the as-deposited samples is an intrinsic property of the $\text{Zn}_{1-x}\text{Co}_x\text{O}$ MSs.

Figures 3(a) and 3(b) show the Kerr effect spectra of the annealed samples with different compositions. After annealing, the shapes of the Kerr effect spectra are quite different from those of the as-deposited samples. In Fig. 3(a), θ_k of $\text{Zn}_{0.19}\text{Co}_{0.81}\text{O}$ is enhanced in the low photon energy region (1.7–2.5 eV) and decreases with increasing photon energy. θ_k of $\text{Zn}_{0.28}\text{Co}_{0.72}\text{O}$ is enhanced in the region of 2.5–3.2 eV and shows a Kerr rotation peak at about 2.95 eV with the maximum value of 0.39° . Especially, θ_k of $\text{Zn}_{0.44}\text{Co}_{0.56}\text{O}$ is largely enhanced in a broad region of 2.0–3.2 eV and a maximum θ_k of 0.72° is obtained at 2.65 eV. In Fig. 3(b), η_k of $\text{Zn}_{0.19}\text{Co}_{0.81}\text{O}$ increases slightly with increasing photon energy, and the negative peaks of η_k change to 2.6 and 2.25 eV for $\text{Zn}_{0.28}\text{Co}_{0.72}\text{O}$ and $\text{Zn}_{0.44}\text{Co}_{0.56}\text{O}$, respectively. θ_k of hcp and fcc cobalt films are both less than 0.6° in a wide photon energy region of 0–6 eV.¹¹ In Co/Pt multilayers^{12,13} and CoPt alloy films,^{9,14} the maximal values of θ_k are 0.55° and 0.6° , respectively, in the visible light region. And in Co/Ag/Pt(001) trilayers θ_k reaches 0.4° at 632.8 nm.¹⁵ θ_k of 0.72° is obviously larger than that obtained in pure cobalt, Co/Pt multilayers, Co/Ag/Pt trilayers, and CoPt alloy films. θ_k in the region of 2.4–3.0 eV including the blue light region is larger than 0.5° , which offers potential promise for the magneto-optical applications in short light wavelength.

The polar Kerr rotation θ_k and Kerr ellipticity η_k are generally expressed as¹⁶

$$\theta_k + i\eta_k = \frac{-\varepsilon_{xy}}{(\varepsilon_{xx} - 1)\sqrt{\varepsilon_{xx}}}, \quad (1)$$

where $\varepsilon_{xx} = (n + ik)^2$ is the diagonal term and $\varepsilon_{xy} = \varepsilon_{xy1} + i\varepsilon_{xy2}$ is the off-diagonal term of the complex dielectric tensor, n and k are optical constants, and ε_{xy1} is the real part and ε_{xy2} is the imaginary part of the off-diagonal term. Since the an-

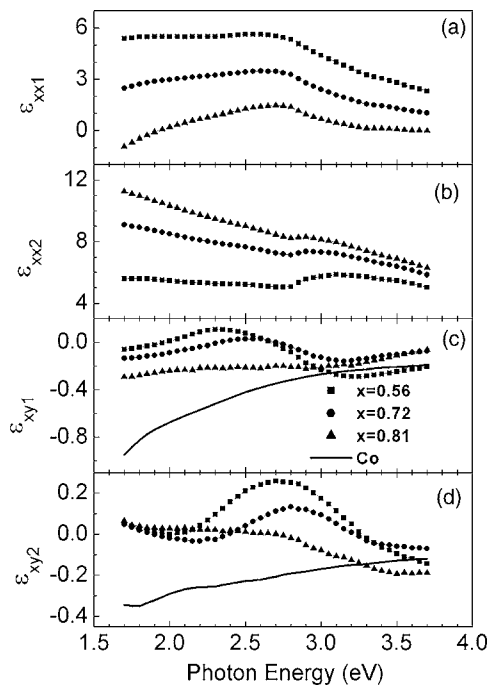


FIG. 4. The real part ϵ_{xx1} (a) and imaginary part ϵ_{xx2} (b) of ϵ_{xx} and the real part ϵ_{xy1} (c) and imaginary part ϵ_{xy2} (d) of ϵ_{xy} for annealed $\text{Zn}_{1-x}\text{Co}_x\text{O}$ MS samples. ϵ_{xy} of pure Co is added for comparison (solid line).

annealed samples can be regarded as a nanocomposite system consisting of ferromagnetic Co clusters and remanent $\text{Zn}_{1-x}\text{Co}_x\text{O}$ matrix, the Kerr rotation of the annealed samples is the combining effects from both ferromagnetic Co clusters and remanent $\text{Zn}_{1-x}\text{Co}_x\text{O}$ matrix, and an enhancement in the Kerr rotation may occur after a proper annealing as compared with the as-deposited samples. Therefore, the Kerr spectra of the annealed samples were further analyzed by the effective medium theory¹⁷ and Eq. (1). First, according to the effective medium theory,¹⁷ the effective diagonal term of dielectric tensor ϵ_{xx} can be obtained by using the optical constants of Co metal¹⁸ and the remanent $\text{Zn}_{1-x}\text{Co}_x\text{O}$ matrix. Taking into account the solubility of Co in ZnO in the thermal equilibrium state,⁸ the optical constants of the $\text{Zn}_{1-x}\text{Co}_x\text{O}$ with $x=0.22$ (Ref. 19) were adopted for the remanent $\text{Zn}_{1-x}\text{Co}_x\text{O}$ matrix. Then the effective off-diagonal term of the dielectric tensor ϵ_{xy} was extracted according to Eq. (1) by using the experimental data in Fig. 3 and the calculated ϵ_{xx} . However, since the dielectric tensor ϵ_{xy} of the remanent $\text{Zn}_{1-x}\text{Co}_x\text{O}$ matrix was not available beforehand, a quantitative simulation of the enhanced Kerr rotation by the effective medium model could not be done on the annealed samples.

Figures 4(a)–4(d) show ϵ_{xx} and ϵ_{xy} spectra of annealed $\text{Zn}_{1-x}\text{Co}_x\text{O}$ MS films with different compositions. In Figs. 4(a) and 4(b), the dependence of ϵ_{xx} (ϵ_{xx1} and ϵ_{xx2}) on the photon energy is similar for the annealed samples of different compositions although ϵ_{xx} varies monotonously with the compositions. In Fig. 4(c), ϵ_{xy1} is larger than that of pure Co especially in the low photon energy region and it tends to decrease while the Co concentration increases. In Fig. 4(d), the spectral dependence of ϵ_{xy2} is similar to that of the Kerr rotation in Fig. 3(a). ϵ_{xy2} shows wide peaks around 2.85 and 2.7 eV for $\text{Zn}_{0.28}\text{Co}_{0.72}\text{O}$ and $\text{Zn}_{0.44}\text{Co}_{0.56}\text{O}$, respectively, which nearly respond to their Kerr rotation peaks. In this

case, the wide peak of the enhanced Kerr rotation in the annealed samples is mainly related to the wide peak of ϵ_{xy2} .

It was found that the transparent $\text{Zn}_{1-x}\text{Co}_x\text{O}$ diluted magnetic semiconductor showed large magneto-optical effects near the optical absorption edge due to the interband transition.⁶ In our case, $\text{Zn}_{1-x}\text{Co}_x\text{O}$ MSs are half transparent and show significant optical absorption in a wide photon energy range due to the interband transitions. Since the dielectric tensor is determined by the interband and intraband transitions, the interband transitions in a wide photon energy range can greatly change the dielectric tensor of the $\text{Zn}_{1-x}\text{Co}_x\text{O}$ matrix. According to the effective medium theory, the effective dielectric tensor of the annealed samples can be greatly modified by the interband transitions in a wide photon energy range, and thus a large magneto-optical effect may occur in the optical absorption region for the annealed samples.

In summary, the polar magneto-optical Kerr effect in the inhomogeneous $\text{Zn}_{1-x}\text{Co}_x\text{O}$ MSs has been studied at room temperature. The polar Kerr rotation of the samples is compositional dependent and enhanced largely after annealing. The maximal Kerr rotation, 0.72° , observed at room temperature for the annealed sample is higher than that of pure cobalt, Pt/Co multilayers, and $\text{Pt}_x\text{Co}_{1-x}$ alloys. The enhanced Kerr rotation in the annealed samples can be explained by the fact that the annealed samples became a nanocomposite system consisting of ferromagnetic Co clusters and $\text{Zn}_{1-x}\text{Co}_x\text{O}$ magnetic semiconductor.

This work was supported by the Project 973 Grant No. 2001CB610603, NCET040634 and NSF Grant Nos. 10234010, 50102019, and 50572053.

¹H. Ohno, *Science* **281**, 951 (1998).

²H. Ohno and F. Matsukura, *Solid State Commun.* **117**, 179 (2001).

³S. S. Yan, C. Ren, X. Wang, Y. Xin, Z. X. Zhou, L. M. Mei, M. J. Ren, Y. X. Chen, Y. H. Liu, and H. Garmestani, *Appl. Phys. Lett.* **84**, 2376 (2004).

⁴D. P. Norton, M. E. Overberg, S. J. Pearton, K. Pruessner, J. D. Budai, L. A. Boatner, M. F. Chisholm, J. S. Lee, Z. G. Khim, Y. D. Park, and R. G. Wilson, *Appl. Phys. Lett.* **83**, 5488 (2003).

⁵H. J. Lee, S. Y. Jeong, C. R. Cho, and C. H. Park, *Appl. Phys. Lett.* **81**, 4020 (2002).

⁶K. Ando, H. Saito, Z. Jin, T. Fukumura, M. Kawasaki, Y. Matsumoto, and H. Koinuma, *Appl. Phys. Lett.* **78**, 2700 (2001).

⁷K. Ando, H. Saito, Z. Jin, T. Fukumura, M. Kawasaki, Y. Matsumoto, and H. Koinuma, *J. Appl. Phys.* **89**, 7284 (2001).

⁸Z. Jin, T. Fukumura, M. Kawasaki, K. Ando, H. Saito, T. Sekiguchi, Y. Z. Yoo, M. Murakami, T. Hasegawa, and H. Koinuma, *Appl. Phys. Lett.* **78**, 3824 (2001).

⁹B. M. Lairson and B. M. Clemens, *Appl. Phys. Lett.* **63**, 1438 (1993).

¹⁰J. M. MacLaren and W. Huang, *J. Appl. Phys.* **79**, 6196 (1996).

¹¹T. Suzuki, D. Weller, C. A. Chang, R. Savoy, T. Huang, B. A. Gurney, and V. Speriosu, *Appl. Phys. Lett.* **64**, 2736 (1994).

¹²P. F. Garcia, M. Reilly, W. B. Zeper, and H. W. V. Kesteren, *Appl. Phys. Lett.* **58**, 191 (1991).

¹³S. Uba, L. Uba, A. N. Yaresko, A. Y. Perlov, V. N. Antonov, and R. Gontarz, *Phys. Rev. B* **53**, 6526 (1996).

¹⁴L. Uba, S. Uba, V. N. Antonov, A. N. Yaresko, and R. Gontarz, *Phys. Rev. B* **64**, 125105 (2001).

¹⁵C. W. Su, C. L. Tzeng, H. Y. Ho, and C. S. Shern, *J. Appl. Phys.* **94**, 5873 (2003).

¹⁶P. N. Argyres, *Phys. Rev.* **97**, 334 (1955).

¹⁷D. Stroud, *Phys. Rev. B* **12**, 3368 (1975).

¹⁸P. B. Johnson and R. W. Christy, *Phys. Rev. B* **9**, 5056 (1974).

¹⁹K. J. Kim and Y. R. Park, *Appl. Phys. Lett.* **81**, 1420 (2002).